Mutations in *filamin 1* Prevent Migration of Cerebral Cortical Neurons in Human Periventricular Heterotopia

Jeremy W. Fox,[1,2] Edward D. Lamperti,[1]
Yaman Z. Ekşioğlu,[3] Susan E. Hong,[1] Yuanyi Feng,[1]
Donna A. Graham,[1] Ingrid E. Scheffer,[4]
William B. Dobyns,[5] Betsy A. Hirsch,[6]
Rodney A. Radtke,[7] Samuel F. Berkovic,[4]
Peter R. Huttenlocher,[8] and Christopher A. Walsh[1,2,9]
[1]Division of Neurogenetics
Department of Neurology
Beth Israel Deaconess Medical Center
Harvard Institutes of Medicine
[2]Program in Biological and Biomedical Sciences
Harvard Medical School
Boston, Massachusetts 02115
[3]Department of Neurology
Massachusetts General Hospital
Charlestown, Massachusetts 02129
[4]Department of Neurology
University of Melbourne
Austin and Repatriation Medical Centre
3084 Heidelberg
Australia
[5]Departments of Human Genetics, Neurology,
  and Pediatrics
[6]Department of Laboratory Medicine and Pathology
University of Minnesota
Minneapolis, Minnesota 55455
[7]Division of Neurology
Duke University Medical Center
Durham, North Carolina 27710
[8]Department of Pediatrics
University of Chicago
Chicago, Illinois 60637

Summary

Long-range, directed migration is particularly dramatic in the cerebral cortex, where postmitotic neurons generated deep in the brain migrate to form layers with distinct form and function. In the X-linked dominant human disorder periventricular heterotopia (PH), many neurons fail to migrate and persist as nodules lining the ventricular surface. Females with PH present with epilepsy and other signs, including patent ductus arteriosus and coagulopathy, while hemizygous males die embryonically. We have identified the PH gene as *filamin 1* (*FLN1*), which encodes an actin-cross-linking phosphoprotein that transduces ligand–receptor binding into actin reorganization, and which is required for locomotion of many cell types. *FLN1* shows previously unrecognized, high-level expression in the developing cortex, is required for neuronal migration to the cortex, and is essential for embryogenesis.

Introduction

The migration of neurons into the mammalian cerebral cortex provides an excellent system for genetic study

of directed cellular migration. Neurons of the cerebral cortex are not generated in situ but instead arise in a specialized germinal zone deep in the brain, called the ventricular zone, and must migrate as many as thousands of cell body lengths into the region of the future cortex. This migration is highly specific, as neurons navigate to predetermined locations that define the six functional layers of the adult cerebral cortex. The migration of cortical neurons has been exhaustively characterized, and several human and mouse mutations disrupt this migration in defined ways. For example, in the *reeler* (Caviness and Sidman, 1973) and *scrambler* (Gonzalez et al., 1997) mutant mice, and in mice with engineered mutations in *cyclin-dependent kinase 5* (*cdk5*) (Ohshima et al., 1996) and its regulator *p35* (Chae et al., 1997), neurons migrate into the cortex but are layered in a fashion that is approximately inverted relative to normal. In the human double cortex syndrome (des Portes et al., 1998; Gleeson et al., 1998) and the human lissencephalic disorders (Reiner et al., 1993), some or all cortical neurons arrest roughly halfway between where they are formed and where they belong. The signaling pathways defined by these several genes remain quite uncertain, however, principally because the receptors and biochemical targets of the identified signaling proteins are both unknown.

Whereas mutant neurons in the genetic disorders listed above show some preserved neuronal migration, suggesting that the migratory machinery is basically intact, another disorder in which neuronal migration completely fails, called periventricular heterotopia (PH), may identify a component essential for neuronal migration (Ekşioğlu et al., 1996). In PH, subsets of neurons fail to migrate into the developing cerebral cortex and remain as nodules of neurons that line the ventricular surface (Figure 1). PH is an X-linked dominant disorder that presents primarily in females (Huttenlocher et al., 1994; Ekşioğlu et al., 1996). Therefore, the neurons that fail to migrate are likely to represent those cells that, due to X inactivation, express genes from the X chromosome that carries the mutated copy of the PH gene. Remarkably, most females with PH show normal intelligence but suffer from seizures and pleiomorphic extra-CNS signs, especially relating to the vascular system (Huttenlocher et al., 1994; Ekşioğlu et al., 1996). Most males with PH gene mutations die during early embryogenesis (Ekşioğlu et al., 1996), and it has been hypothesized that the PH gene also has essential functions in developing nonneural tissues.

Here, we show that PH reflects spontaneous, de novo, intragenic mutations in a single gene, *filamin 1* (*FLN1*, also known as *nonmuscle filamin*, *actin binding protein 280,* and *ABP-280*), and detail the CNS and extra-CNS phenotypes of *FLN1* mutations. FLN1 is a 280 kDa actin-cross-linking phosphoprotein originally isolated from motile blood cells and subsequently shown to be expressed in many nonmuscle cells (Hartwig et al., 1980; Hartwig and Shevlin, 1986; Gorlin et al., 1990; Hartwig, 1992). FLN1 has been shown to be essential for migration in melanocytes and other cultured cells by in vitro

[9]To whom correspondence should be addressed (e-mail: cwalsh@bidmc.harvard.edu).
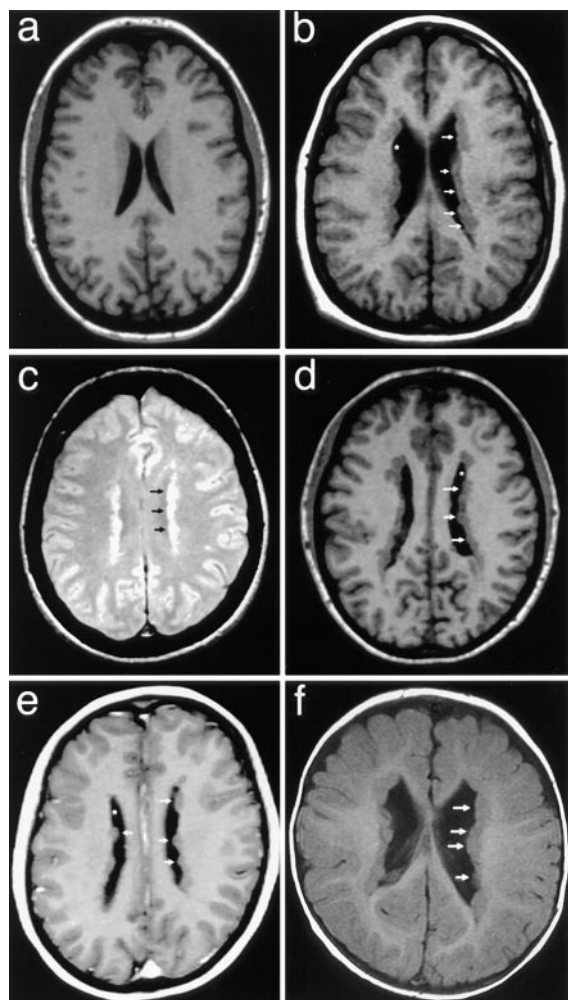
Figure 1. Anatomical Phenotype of PH with Different *FLN1* Mutations Shows Similar Features

(a) MRI of normal human cortex, performed using T1-weighting and formatted in the axial plane, showing normal ventricles with normally smooth ventricular epithelium.

(b) MRI formatted in a similar plane and with similar technique, showing the affected mother from pedigree 2 (Figure 3b).

(c) Axial MRI of affected female III-10 from pedigree 1 (Figure 3a). MRI was formatted in the same plane, but with greater T2-weighted technique, so that the gray matter now appears brighter white than gray matter in (a) and (b).

(d–f) Axial MRI of sporadic patients from Figure 3e, Figure 3c, and Figure 3d, respectively, taken with technique and formatting similar to (a) and (b). MRI of each of the five PH brains (all showing distinct *FLN1* mutations) show somewhat enlarged ventricles and near-continuous bilateral lining of ectopic gray matter nodules (arrows). For comparison, ventricular surfaces free from heterotopias are marked with asterisks.

genetic and cellular studies (Stendahl et al., 1980; Cunningham et al., 1992). FLN1 appears to directly link membrane receptors to the actin cytoskeleton, to regulate the formation of actin stress fibers and adhesive contacts, and to bind several other crucial regulators of the cytoskeleton such as SEK-1 and Trio (Matsudaira, 1994; Marti et al., 1997; Bellanger et al., 1998). However, the in vivo effects of loss of FLN1 function have never been known, and a role for FLN1 in migrating neurons was

never suspected. Here, we show that FLN1 is particularly enriched in the brain during the period of most active neuronal migration and then is downregulated in the adult. Our data also suggest that FLN1 is essential for normal embryonic development and may have essential roles in developing blood vessels.

Results

Genetic and Physical Mapping of the PH Locus

We previously mapped the PH gene to the distal long arm of the X chromosome (Xq28) with a candidate interval of ~6.5 Mbp from the marker DXS1113 to the subtelomeric, pseudoautosomal region of Xq28 (Ekşioğlu et al., 1996) (Figure 2a). We refined this interval further by reexamining at higher marker resolution our most informative recombination event in a PH patient who carried unaffected alleles for DXS1113 and centromeric markers (patient III-2; Figure 1d in Ekşioğlu et al., 1996). The informative pedigree was reanalyzed with the additional published markers DXS1176 (GDB number 207343), DXS15 (GDB number 207346), and BGN (Just et al., 1994) (Figure 2a). The critical affected individual was recombinant for DXS15 but nonrecombinant for BGN, ~100 kbp distal to DXS15, and was also nonrecombinant for all markers distal to BGN. These data place the crossover event between DXS15 and BGN and reduce the PH candidate interval to ~1 cM (~2.5 Mbp) between DXS15 and the pseudoautosomal region of Xq28 (Figure 2a).

Subsequent analysis of a large duplication of Xq28 in a male PH patient (Fink et al., 1997) with a severe, albeit nonlethal, phenotype allowed the candidate interval to be refined even further, on the hypothesis that this patient was affected due to duplication or disruption of the PH gene. Quantitative Southern blotting (Figures 2b and 2d), confirmed by FISH analysis (data not shown), defined the approximate centromeric border of the duplication. Identification of novel restriction fragments (Figure 2c), followed by linker-mediated PCR amplification and DNA sequencing of the junction fragments (J. W. F., E. D. L., W. B. D., C. A. W., and B. A. H, unpublished data), defined the exact centromeric boundary of the duplicated segment of Xq28 as base 3377 of 3395 of intron 1 of the *isocitrate dehydrogenase* gene (*IDH*), ~600 kbp distal to DXS15. However, none of the genes identified at the breakpoints or insertion site of the duplication harbored independent mutations in other PH patients. Therefore, we concluded that the duplication itself was responsible for PH in this patient. This patient redefined the likely PH gene region as between *IDH* and the pseudoautosomal region, a distance of ~1.9 Mbp.

Candidate Gene Analysis of PH

Having narrowed the PH candidate interval, we moved next to candidate gene analysis. Because distal Xq28 is extremely gene dense, with a number of human diseases mapping to this area, a substantial fraction of the 1.9 Mbp PH candidate region has been completely sequenced (Figure 2). The sequenced area distal to *IDH* covers 643 kbp (GenBank accession numbers U52111,
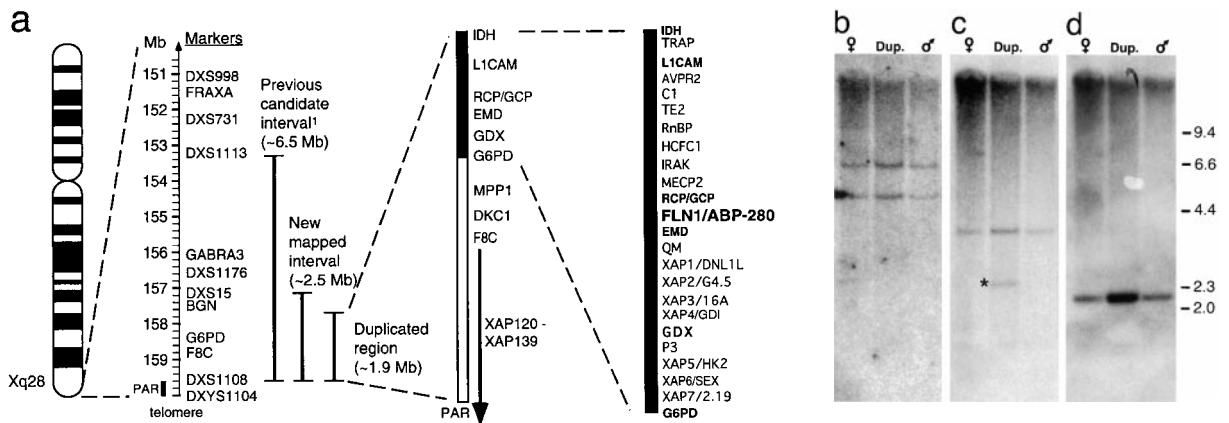
Figure 2. Genetic and Physical Mapping of PH Locus

(a) The 6.5 Mbp "previous candidate interval" was defined by a recombination event between the DXS1113 marker and the PH locus (Ekşioğlu et al., 1996). This informative recombination event was further characterized with additional markers including DXS15 and BGN. The recombination event occurred between these two markers, and the candidate interval was thus refined to distal of DXS15 ("new mapped interval"). The identification of the proximal boundary of a chromosomal duplication in an additional PH patient allowed the PH candidate interval to be further narrowed to include only those genes telomeric to the *isocitrate dehydrogenase* (*IDH*) gene. All characterized genes in the candidate region are shown. The distal boundary of the candidate interval is the pseudoautosomal region (PAR). The 643 kbp of Xq28 that is fully sequenced is depicted in black.

(b–d) The definition of the proximal boundary of the Xq28 duplication using Southern blot analysis. All three panels show sequential Southern hybridization with three different probes to the same filter, containing DNA isolated from the mother of a male with periventricular heterotopia, both of whom carry a duplication of distal Xq28 (labeled "dup") (Fink et al., 1997). Hybridization to a PCR-generated probe from the region of the *PLEXR* gene (Figure 2b), not duplicated, shows equal in a normal female (lane 1), the patient with the duplication (lane 2), and a normal male. Two bands are seen in the normal state since the probe spans a restriction site. Hybridization to a probe generated from the *IDH* gene (at the centromeric border of the duplication) shows normal bands in lanes 1 and 3 and a normal band (from the normal X chromosome in this female carrying the duplication) and an abnormal junction fragment in lane 2 (Figure 2c, marked by an asterisk). Similar abnormal fragments were seen with five different restriction enzymes and confirmed by PCR amplification and direct sequencing of the junction site. Hybridization to a third, more distal, duplicated probe from the region of *G6PD* (Figure 2d) shows increased hybridization in the female carrying the duplication. These hybridization findings were consistent and reproducible with multiple probes and confirmed by dosage analysis with FISH.

U52112, AF030876, Z47046, Z47066, Z68193, Z46936, Z49258, and L44140) and contains 23 characterized genes. The ~1.2 Mbp unsequenced area telomeric to the 643 kbp sequenced block has a lower gene density but still harbors at least a dozen additional genes, though most are incompletely characterized (Rogner et al., 1996). More than half of the genes in the PH candidate interval are expressed at some detectable level in brain and thus were formally candidates for the PH gene. Candidate genes were tested in PH patients by Southern blotting to search for gross rearrangements, and/or performing single-stranded conformational polymorphism analysis (SSCP) to search for intragenic point mutations. A partial list of candidate genes tested includes *XAP3* (Sedlacek et al., 1993), *XAP4* (also known as *Rab3a GTPase dissociation inhibitor*, and subsequently found to be mutated in nonsyndromic X-linked mental retardation) (D'Adamo et al., 1998), *XAP5*, *XAP6* (Maestrini et al., 1996), *XAP7*, *MPP1*, *CDM*, *PMCA3*, *IDH*, *TRAP*, and *PLEXR*. While several benign sequence polymorphisms or restriction fragment length polymorphisms were discovered in some of these genes, none of them harbored any mutations in PH patients. In contrast, *FLN1* immediately showed multiple deleterious mutations by SSCP analysis and DNA sequencing.

FLN1 Mutations in PH

FLN1 consists of 48 exons covering 26 kbp of genomic sequence and has a 7.9 kb open reading frame (ORF)

(Patrosso et al., 1994). The gene is adjacent to the *emerin* gene (which causes Emery-Dreyfuss muscular dystrophy, EDMD), and the two genes are flanked by inverted repeats, causing the genomic segment containing these two genes to be present in two orientations in the population at large (Small et al., 1997). All large scale rearrangements of *emerin* associated with EDMD had notably failed to include *FLN1*, suggesting that loss of FLN1 function might be embryonically lethal (Small and Warren, 1998). *FLN1* was tested as a candidate gene for PH in 25 females (representing either sporadic cases or representatives of distinct pedigrees) by PCR amplifying genomic DNA from single exons and analyzing the products by SSCP. Screening of exons 2–5, representing the first four coding exons (11% of the full ORF) and encoding the actin-binding domain (Patrosso et al., 1994), alone showed several point mutations, which are described here. In SSCP analysis, aberrantly migrating bands were observed in five unrelated patients (Figure 3) for exons 2–5. Normal and aberrant bands were eluted from the gels, reamplified, and sequenced alongside normal controls as well as the original heterozygous PCR products used for the SSCP analysis. When appropriate, all available family members were amplified and analyzed similarly (Figures 3a and 3b). Each aberrant band was found to represent a loss-of-function mutation upon DNA sequence analysis.

In the largest reported PH pedigree (Huttenlocher et al., 1994), we found a C to T substitution in exon 3 (Figure
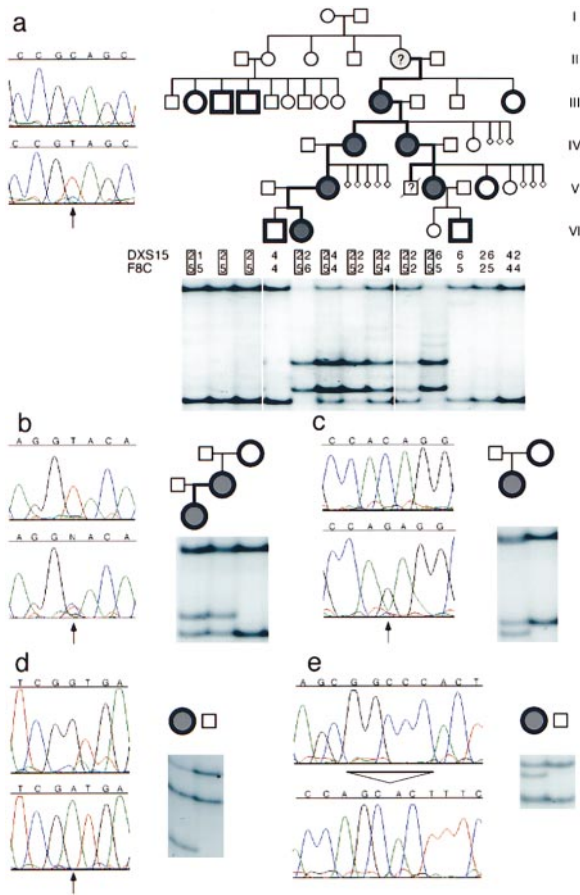
Figure 3. *FLN1* Mutations in PH Patients

Affected patients are shaded, and individuals genotyped and analyzed by SSCP are large and bold. SSCP results are presented directly below screened individuals.

(a) The largest reported PH pedigree (Huttenlocher et al., 1994). Affected females show two additional SSCP bands, indicating heterozygosity for a CAG (Gln) to a TAG (stop) nonsense mutation (shown in chromatogram on left), which truncates the FLN1 protein near the N terminus (amino acid 182 of 2648). The genotype of analyzed individuals for two markers flanking the *FLN1* locus, DXS15 and F8C, are shown. All affected individuals shared the same haplotype at DXS15, F8C, as well as for four other Xq28 markers between them. The mutation arose de novo on the "2,5" chromosome in the germline of either individual I-1, I-2, or II-5, as the mutation is absent from this chromosome in the progeny of II-2 (III-2, III-3, III-4).

(b) A second pedigree with a T to C transition in the consensus splice donor (base 2) of intron 4 (AGgtaca to AGgcaca), shown in its heterozygous state in the chromatogram. This mutation likely arose in the germline of one of the grandparents in this pedigree.

(c) A sporadic PH patient with a C to G substitution at the consensus splice acceptor of intron 3 (3 bases from exon 4, ccacagG to ccagag G). This mutation likely arose in the germline of one of this patient's parents as the mother does not harbor the base change.

(d) A sporadic patient with a G to A change at the consensus splice donor site (base 1) of intron 2 (TCGgt to TCGat). An unrelated control shows the expected pattern of SSCP bands.

(e) A sporadic patient with a 5 base deletion (AGCGGCCCACT to AGC_ACT) in exon 2 with a normal control for comparison.

3a), which converts a CAG (Gln) to a TAG (stop) codon and truncates the FLN1 protein at amino acid residue 182 of 2647 (Figure 3a). The mutation demonstrates perfect segregation with the PH phenotype in all affected

females in the pedigree. Moreover, a distant branch of this same family was available for haplotype analysis using flanking markers and demonstrates the de novo origin of the mutation (Figure 3a). First cousins (III-2, III-3, and III-4) of the oldest known affected female (III-10) share the "affected" haplotype (the chromosome that carries DXS15 allele 2 and F8C allele 5) but do not harbor the *FLN1* mutation and are phenotypically normal. In contrast, all descendants of III-10 who carry the affected haplotype also harbor the nonsense *FLN1* mutation and present with PH.

In a second pedigree, we identified a T to C substitution at the second base of intron 4 (Figure 3b) in the splice donor sequence (AGgtaca to AGgcaca). A "t" at position +2 of the intron is conserved among 100% of vertebrate splice junctions studied (Shapiro and Senapathy, 1987). The mutation is predicted to cause either exon skipping or a read-through of intron 4, which would introduce a stop codon after the translation of 30 additional amino acids. The mutation is present both in a mother and daughter with PH but not in the unaffected maternal grandmother. Therefore, this mutation also most likely arose de novo in this pedigree in the germline of either the maternal grandmother or grandfather, both of whom were clinically unaffected.

Three other mutations were identified in sporadic PH patients. In the first (Figure 3c), the consensus splice acceptor at the end of intron 3 (3 bases from exon 4) is mutated by a C to G substitution (ccacagG to ccagagG). The "c" at position −3 is conserved among >70% of vertebrate splice junctions, and a "g" at this position is only seen in 1% (Shapiro and Senapathy, 1987). The mother of this patient is phenotypically normal and does not harbor the mutant allele. Thus, it is likely that this mutation arose de novo in the germline of the patient's mother or father. The second sporadic mutation (Figure 3d) is a G to A substitution at the first base of intron 2 in the conserved splice donor (TCGgt to TCGat). The "g" at position +1 of the intron is conserved in 100% of splice donor sequences of vertebrate genes (Shapiro and Senapathy, 1987). These two splicing mutations are again predicted to either cause exon skipping or truncation of the FLN1 protein due to a read-through of the respective introns with the introduction of a stop codon. The final sporadic mutation is a 5 base deletion within the coding region of exon 2 (Figure 3e). This deletion removes bases 287–291 of the 7.9 kb ORF (AGCGG CCCACT to AGC_ACT), producing a frame shift and the introduction of a premature stop codon after the addition of 8 inappropriate amino acids.

Expression Pattern of *FLN1* in Developing Brain

Filamin-like immunoreactivity has previously been shown in cultured developing dorsal root ganglion neurons (Letourneau and Shattuck, 1989), suggesting a likely role for FLN1 or a related protein as a cell-autonomous cytoplasmic factor acting in the migrating neuron. Northern analysis had previously shown some *FLN1* expression in brain (Maestrini et al., 1993), though recent immunohistochemical analysis in normal adult human brain showed the expression of FLN1 to be somewhat limited, with most expression restricted to various types of blood
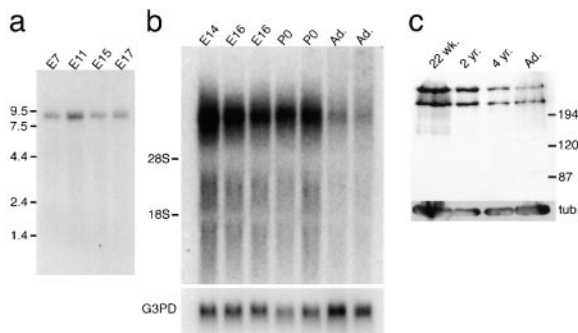
Figure 4. Analysis of *FLN1* Expression

(a) Commercial Northern blot (Clontech, Palo Alto, CA) containing poly(A) selected RNA from total mouse embryos from embryonic day 7, 11, 15, and 17 probed with the *FLN1* 3′ UTR probe. Specificity of the probe is confirmed by the appearance of a single band at 9.0 kb. Expression is highest at E11, at the onset of neuronal migration.
(b) Northern blot of total RNA from brains of mice from E14 and E16, P0, and adult (P99 and P286). *FLN1* message is most abundant at E14, and expression remains high through birth but is strongly downregulated in the adult. The quality of the RNA was checked by direct visualization following ethidium bromide staining and by probing the membrane with a *G3PD* control probe (bottom).
(c) Western analysis of FLN1 expression in human fetal brain (lanes 1 and 2) and postnatal brain. FLN1 appears as two bands that are commonly seen in other Western blots of FLN1 (Loo et al., 1998) and appear to represent alternative splice forms. Expression of FLN1 (compared to a tubulin loading control) decreases substantially during postnatal development.
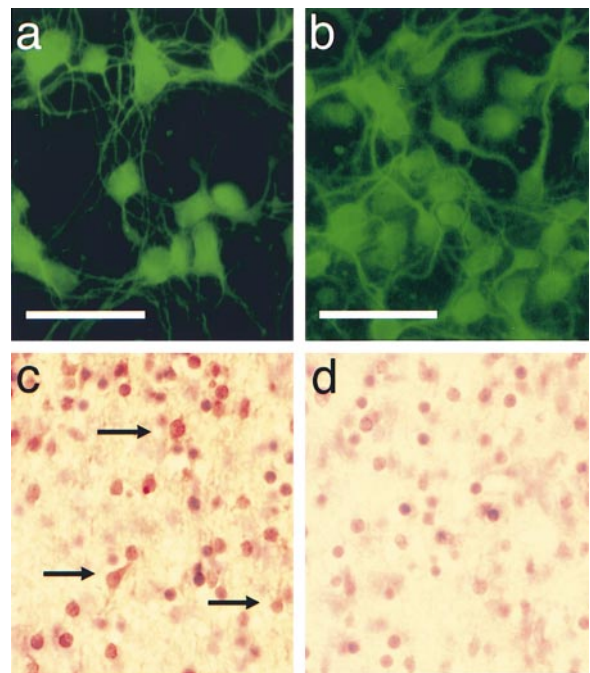

Figure 5. Localization of FLN1 in Cultured Neuronal Cells and in Developing Brain

(a) Immunofluorescence staining of cultured E15 rat hippocampal neurons after 3 days in culture. Stained neurons show FLN1 immunoreactivity throughout their processes, including growth cones.
(b) Similar results were seen using primary mouse cortical cultures and cultured P19 cells differentiated toward neural fates with retinoic acid (data not shown).
Scale bars, 30 μm. Controls lacking primary antibody showed complete absence of staining (data not shown).
(c) Immunohistochemical staining of the intermediate zone of the human cortex at 21–22 weeks gestation, with a hematoxylin counterstain. Stained cells show brown immunoreactivity in the perinuclear region and in some of the radially oriented cytoplasmic processes (arrows), as well as blue hematoxylin counterstain. Arrows, 30 μm.
(d) Negative control (no primary antibody) shows only cells counterstained by the hematoxylin.

vessels (Zhang et al., 1998). We therefore tested whether *FLN1* might be developmentally regulated in the brain, with high expression during the period of neuronal migration and subsequent downregulation. A commercial membrane (Clontech, Palo Alto, CA) containing poly(A) selected RNA from total mouse embryos was hybridized with a probe generated from the 3′ UTR of the mouse *FLN1* message, in order to avoid cross-reactivity with other filamin family members. There was robust expression of a single *FLN1* message (Figure 4a), demonstrating specificity of the probe. In order to examine *FLN1* expression in the developing brain, total RNA from the brains of E14, E16, P0, and adult mice were subjected to Northern analysis using the same probe. Expression of *FLN1* was high at all embryonic time points tested and was still high at birth, but by adulthood (P99) *FLN1* expression was reduced by at least an order of magnitude (Figure 4b). These Northern results show that *FLN1* is indeed developmentally regulated in brain with high expression during the period of cortical neuronal migration (E12–P8 in the mouse) followed by marked downregulation. Western blot analysis of FLN1 in the developing human brain using a monoclonal antibody raised to FLN1 (Serotec, Raleigh, NC) showed the presence of two isoforms (Figure 4c) that have been previously observed and thought to represent alternative splice forms (Loo et al., 1998). The level of FLN1 protein is again high in human fetal brain, with lower expression at postnatal ages (Figure 4c).

Immunofluorescence analysis of neuronal cultures using a second monoclonal antibody raised to FLN1 (Chemicon International, Temecula, CA) demonstrated robust FLN1 localization in embryonic neurons, as well

as showing lower amounts of expression in glial cells. Cultured embryonic (E15) rat hippocampal neurons showed robust FLN1 immunoreactivity (Figure 5a) that was particularly striking in the neurites and growth cones. Primary cultures of mouse cortex at E15 also showed robust staining of neurons and their neurites and growth cones (Figure 5b). Cultured P19 cells differentiated toward neural fates using retinoic acid also showed intense FLN1 immunoreactivity throughout the somata and neuritic processes of neuron-like cells (data not shown). Some FLN1 immunoreactivity was also seen in cultured mouse glial cells and in the flat cells in the P19 cultures, which are likely to be glial, so that a role for FLN1 in glia cannot be ruled out.

Immunohistochemical analysis confirmed that FLN1 is expressed in the developing brain predominantly in migrating and postmigratory neurons. Human embryonic brain at 21–22 weeks gestation (a period after most neurogenesis is complete, but while many neurons are still migrating to the cortex) showed FLN1 expression in bipolar cells of the cortical plate whose morphology

and location were highly suggestive of neuroblasts (data not shown). In the intermediate zone, expression was also seen in the cytoplasm of cells that matched the morphology of radially migrating neurons (Figure 5c), suggesting that neurons express FLN1 during radial migration. Negative controls (lacking primary antibody but with hematoxylin counterstain) confirmed the specificity of staining (Figure 5d). Strong FLN1 immunoreactivity was not obvious in glial cells, though lower levels of expression cannot be ruled out.

Non-CNS Phenotypes in Patients with *FLN1* Mutations

In light of the identification of *FLN1* mutations in PH, we reviewed clinical histories and discovered a number of additional congenital anomalies common to patients with *FLN1* mutations (Table 1). For example, 3 of 11 affected females (showing three distinct mutations) were born with patent ductus arteriosus requiring surgical correction, which has a normal incidence of 1/1500 live births (Murray, 1997). In addition, 3 of 11 females with PH suffered strokes at young ages, whereas unaffected females in the same pedigrees showed none. One affected female and the male carrying the Xq28 duplication both had shortened digits, with the male also showing syndactyly and clinodactyly. Other CNS malformations included decreased size of the corpus callosum and a cerebellar anomaly described as an enlarged cisterna magna or cerebellar cyst, but which may represent cerebellar hypoplasia. Other malformations noted in additional females with PH (in which *FLN1* mutations have not yet been determined), particularly the high incidence of patent ductus arteriosus, are consistent with the findings in patients with confirmed mutations. Clinical phenotypes in males with *FLN1* mutations are more difficult to elucidate because of the early lethal phenotype. Interestingly, in the pedigree illustrated in Figure 2a, one male descendant of an affected female (V-3) who carried the disease-linked haplotype was born alive (Figure 2a) but died from severe systemic bleeding and organ failure 3 days later. On postmortem examination, there was severe arrest of myeloid and erythroid differentiation in bone marrow and lymphoid depletion of the thymus.

X Inactivation Analysis in *FLN1* Mutations

Given the embryonic lethality of males with *FLN1* mutations, and the potential requirement for FLN1 in development of some immune cells, we performed X inactivation studies in female patients with confirmed *FLN1* mutations to determine whether FLN1 is required in a cell-autonomous fashion for survival of nucleated peripheral blood cells (Figure 6). Three patients from the largest pedigree (Figure 3a) were analyzed for patterns of X inactivation using the HUMARA marker (Kopp et al., 1997). One patient (III-10) was informative for HUMARA and showed expression from both the X chromosome carrying the *FLN1* mutation and from the normal X chromosome (Figure 6). Another affected female from the same pedigree (V-2) was not informative for HUMARA; however, the affected daughter of V-2 (VI-2) showed

Table 1. Phenotypes in Patients with Documented *FLN1* Mutations

Patients	Number Affected
Heterozygous Females	
Vascular/coagulation	
Stroke before age 60	2
Stroke before age 20	1
Cardiac and major vessel	
Patent ductus arteriosus	3
Bicuspid aortic valve	1
Gastrointestinal	
GI motility defects	1
Extremities	
Shortened digits	1
Neurological	
Congenital strabismus	2
Small corpus callosum	3
Cerebellar abnormality	4
Hemizygous Male	
Vascular/coagulation	
Lethal neonatal hemorrhage	
Immunologic	
Maturation arrest of bone marrow (erythroid and myeloid)	
Lymphoid depletion of thymus	
Male with Large Duplication and PH	
Immunologic	
Immune compromise with recurrent infections	
Extremities	
Syndactyly	
Shortened fingers	
Clinodactyly	
Neurological	
Small corpus callosum	
Hypoplastic cerebellum	

A compilation of phenotypes in 11 females with confirmed point mutations in *FLN1*, one male born alive with a point mutation in *FLN1*, and one male with a large duplication of the *FLN1* region. Affected females (total number = 11 patients, including 8 cases from pedigrees plus three sporadic cases) showed a substantial number of patent ductus arteriosus (3 of 11 cases, versus a population incidence of PDA = 1 per 1500 live births), bicuspid aortic valve (1 of 11 cases, versus a population incidence of 1 per 100 births), and strokes at early ages (3 of 11). An affected male born carrying a presumed complete loss-of-function mutation (a CAG to TAG mutation creating a premature termination codon) also showed overwhelming hemorrhage and arrested myeloid and erythroid bone marrow development. A male showing a duplication of ~2.5 Mbp of DNA, including much of distal Xq28 in addition to *FLN1*, showed several features, but some features may have reflected effects of other genes included in the duplication.

strongly preferential expression of the chromosome inherited from the mother, *carrying the FLN1 mutation* (upper band in VI-2 lane). This is reflected by digestion of the larger allele by HpaII and failure of PCR amplification of this unmethylated, transcriptionally active allele. In contrast, the paternally inherited allele (lower band in VI-2) was preferentially inactivated and hence was not digested by HpaII and was successfully PCR amplified. Analysis of another mother and daughter pair with a different mutation (Figure 3b and "D" and "M" in Figure 6) showed fairly even inactivation of the normal and
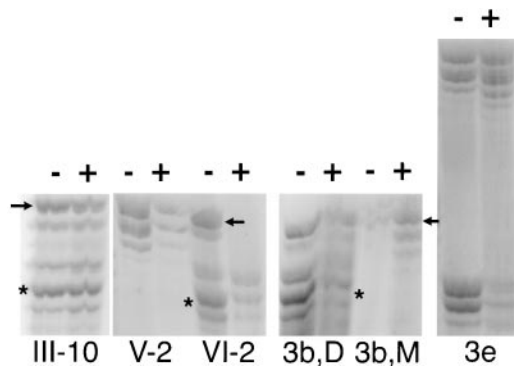
Figure 6. X Inactivation Patterns in Several Individuals and Pedigrees with *FLN1* Mutations Are Not Consistently Biased

The figure shows analysis of the HUMARA marker, performed according to standard techniques (Kopp et al., 1997). Each pair of lanes represents paired experiments in the absence (−) or presence (+) of HpaII, a methylation-sensitive enzyme that preferentially cleaves nonmethylated sequences within the polymorphic HUMARA marker. Paternal alles are marked with an asterisk and maternal alleles are marked with an arrow, except in "3e," as this determination is not possible. The intensity of the two specific bands roughly reflects the balance of X inactivation among peripheral blood nucleated cells, with the polymorphic allele from the transcriptionally active X chromosome being preferentially digested by HpaII ("+" lane in each pair of lanes) and hence not amplified. There appears to be no systematic bias in the balance of X inactivation. Affected patient III-10 from the pedigree shown in Figure 3a is informative for the HUMARA marker but shows no clear skew in X inactivation. V-2 is not informative; her daughter is informative, however, and preferentially inactivates the paternal allele, suggesting that her X inactivation is heavily skewed (as are about 10% of normal females) but actually skewed so that cells expressing the mutant X chromosome predominate. Other patients (3b and 3e) showed modest skewing or balanced X inactivation or were not informative. Since there is no consistent inactivation of the mutant X chromosome, FLN1 does not appear to be required in a cell-autonomous fashion for peripheral mononuclear cell survival.

abnormal chromosomes in the daughter, while a sporadic case (Figure 3e and "3e" in Figure 6) also showed fairly equal expression of both X chromosomes in peripheral nucleated cells. Analysis of 15 other cases of PH in which the specific mutation was not determined also failed to show preferential X inactivation. Since X chromosomes carrying the *FLN1* mutation are not preferentially Lyonized in nucleated circulating blood cells, FLN1 is therefore not required in a cell-autonomous fashion for survival of mixed peripheral white blood cells. However, an essential cell-autonomous role for FLN1 in a subset of nucleated cells or nonnucleated cells (e.g., platelets) cannot be excluded, nor can a possible non-cell-autonomous role for FLN1.

Discussion

Here, we describe the genetic basis for a new multi-organ syndrome due to mutations in the human *FLN1* gene. We show multiple independent *FLN1* mutations with a similar neurological phenotype and, in two pedigrees, demonstrate the de novo origin of the mutations as well as linkage between the mutation and the disease after the mutation arises. Strikingly, the major signs of *FLN1* mutations are seen in heterozygous females, and

the major manifestations are neurological, since males with hemizygous *FLN1* mutations are usually embryonic lethal. The CNS phenotype has major implications for the control of neuronal migration, since FLN1 presents a likely scaffold and target for multiple cytoplasmic signaling proteins that have previously been shown to control the direction and target selection of migrating neurons. First, we will discuss the implication of *FLN1* mutations for previously suspected roles of FLN1 in nonneuronal cells, and then we will take up the implications of the previously unsuspected role of FLN1 in neuronal migration.

Properties of FLN1

FLN1 was originally identified as a high molecular weight protein isolated from motile blood cells that caused purified muscle actin to gel and precipitate (Hartwig and Stossel, 1975), and it was subsequently found to be the most abundant and widely distributed member of a family of large actin-binding proteins (Maestrini et al., 1993). Immunofluorescence with antibodies to a similar protein showed localization along actin-rich stress fibers, leading to the name filamin (Wang et al., 1975). FLN1's most notable feature is its dramatic ability to induce perpendicular branching of actin filaments at low concentrations (Gorlin et al., 1990). A FLN homolog has also been identified in *Dictyostelium discoideum* that regulates actin polymerization (Condeelis et al., 1984), as well as in *Drosophila*, where filamin is implicated in the dorsal signaling pathway through interactions with the Toll receptor (Edwards et al., 1997). At least three distinct *filamin* genes are thought to exist in vertebrates, though limited cDNA cloning has hindered careful comparisons of primary structure and expression patterns.

FLN1 encodes a 2647 amino acid polypeptide with three major functional domains (Gorlin et al., 1990). The N-terminal actin-binding domain (ABD) in FLN1 is structurally similar to the ABDs of dystrophin and α-actinin. The bulk of FLN1 forms a semiflexible rod domain composed of 24 repeats, each containing about 96 amino acids. The rod domain is interrupted twice by short sequence inserts of 20–40 residues between repeats 15–16 and 23–24; these regions are postulated to form flexible hinges and are sites of proteolytic cleavage (Gorlin et al., 1990). The C terminus contains a truncated repeat (Figure 7), and this last repeat is the site of dimerization of FLN1 (Gorlin et al., 1990) and is the site through which FLN1 binds to several membrane proteins such as integrin β1 (Loo et al., 1998; Pfaff et al., 1998) and β2 (Sharma et al., 1995; Glogauer et al., 1998), tissue factor (Ott et al., 1998), and presenilin 1 (Zhang et al., 1998). In contrast, another membrane receptor in platelets, glycoprotein Ibα, appears to bind FLN1 through a region that includes repeats 17–19 (Okita et al., 1985; Meyer et al., 1997).

FLN1 is subject to extensive regulation via phosphorylation that alters its subcellular localization and binding to actin as well as to membrane receptors. For example, FLN1 is translocated from the membrane to the cytosol in endothelial cells in response to bradykinin; this translocation is dependent upon calcium/calmodulin-dependent protein kinase II phosphorylation of the C terminus of FLN1 and is inhibited by the cAMP-dependent protein
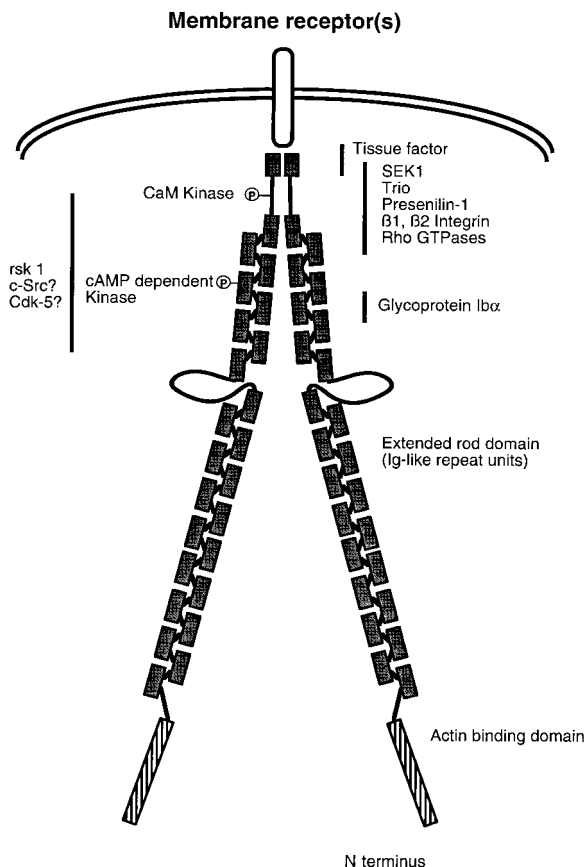
Membrane receptor(s)

Figure 7. Schematic of the Structural Organization of FLN1 as Deduced from Several Sources

The figure shows a FLN1 dimer, including the actin-binding domain (ABD) at the N terminus, the 23 repeats with two hinge regions, one between repeats 15 and 16 and one before repeat 23. Repeat 23 is a truncated repeat, which allows dimerization, and the final repeats also represent the region that binds to several integral membrane proteins including β1 and β2 integrin (Sharma et al., 1995), presenilin 1 (Zhang et al., 1998), and tissue factor in vascular precursor cells (Ott et al., 1998). Binding sites for several other FLN1-binding proteins such as Trio (Bellanger et al., 1998) and SEK-1 (Marti et al., 1997) have not yet been identified. The major membrane receptor bound by FLN1 in platelets is glycoprotein Ibα, which binds a separate site, including repeats 17–19 (Meyer et al., 1997). The two ABD heads associate with F actin and recruit actin filaments to regions of active ligand binding to FLN1-bound receptors (Hartwig et al., 1980; Hartwig and Shevlin, 1986; Gorlin et al., 1990; Hartwig, 1992).

kinase pathway (Gorlin et al., 1990; Wang et al., 1996). Phosphorylation by CaM kinase II also regulates the actin cross-linking activity of another filamin family member (Ohta and Hartwig, 1995).

Non-CNS Roles of FLN1 as Revealed through Mutations

FLN1 has several roles in hemostasis and vascular remodeling that may explain the embryonic lethality of males with *FLN1* mutations, the apparent hypercoagulable state and vascular anomalies of some females with *FLN1* mutations, and the neonatal, fatal bleeding disorder of a single live-born male with a *FLN1* mutation. For example, in vascular cells, FLN1 is the major protein

that binds to tissue factor (TF), the protease receptor for coagulation factor VII that initiates the extrinsic coagulation cascade (Ott et al., 1998). TF also has multiple roles in vascular development, angiogenesis, and tumor cell metastasis for which the mechanisms are poorly defined (Bugge et al., 1996). The intracellular domain of TF binds FLN1, and FLN1 recruitment to TF in response to extracellular ligands is associated with reorganization of actin filaments (Ott et al., 1998). Mice with engineered mutations in TF show virtually 100% embryonic lethality due to widespread hemorrhage (Bugge et al., 1996). TF/FLN1 interactions in vascular remodeling may relate to the elevated incidence of patent ductus arteriosus in females with *FLN1* mutations. The ductus arteriosus, required for the fetal blood circulation, normally closes in the hours and days after birth as the postnatal pattern of blood circulation is established, but in PDA this closure fails.

FLN1 has a second critical link to hemostasis by acting in platelets to couple glycoprotein Ibα, part of the receptor for von Willebrand's factor (vWF) and thrombin involved in platelet aggregation, to the actin cytoskeleton (Okita et al., 1985; Meyer et al., 1997). Binding of vWF to glycoprotein Ibα causes FLN1-modulated spreading of platelets to form a monolayer at the earliest stages of thrombus formation (Murray, 1997); abnormalities of this critical function may contribute either to hypercoagulability (e.g., strokes suffered at young ages by 3 of 11 affected females) or hemorrhagic disorders. Homozygous mutations in the glycoprotein Ibα gene cause a severe bleeding disorder called the Bernard-Soulier syndrome, which is often fatal neonatally (Ware et al., 1990). The single live-born male carrying a *FLN1* mutation who died neonatally of a lethal bleeding disorder thus seems to represent a phenocopy either of the TF mutant phenotype or the Bernard-Soulier syndrome.

Our data provide some evidence for a requirement of FLN1 in immune function, since (1) defects in immune development were seen in the male who died neonatally who carried a *FLN1* point mutation (Table 1), and (2) defects in immune function are present in a male with a duplication of Xq28 that included the *FLN1* locus. Thus, lymphocytes from patients with *FLN1* mutations may have functional defects. However, FLN1 does not appear to be required for survival of all nucleated peripheral blood cells in a simple, cell-autononous fashion, since X inactivation studies in females with *FLN1* mutations failed to show nonrandom patterns of X inactivation in circulating peripheral blood lymphocytes. In principle, cell-autononous requirements for FLN1 function in each component of the peripheral blood (and indeed in each organ) could be studied by sorting individual cell types from affected females and determining patterns of X inactivation.

FLN1 has been previously implicated as essential for the migration of several cell types, notably melanocytes (Cunningham et al., 1992), tumor cells, and leukocytes (Stendahl et al., 1980). Cultured melanocytes that lack FLN1 show defects in pseudopodia formation and abnormal surface blebbing, and these defects are corrected by transfection of *FLN1* cDNA clones (Cunningham et al., 1992). Melanocytes that are deficient in FLN1 also show defects in actin dynamics and are excessively

sensitive to mechanical deformation (Glogauer et al., 1998). Similarly, *Dictyostelium discoideum* that are deficient in the FLN1 homolog ABP-120 show substantial defects in actin cross-linking, pseudopod extension, cytoskeletal structure, cell motility, chemotaxis, and phagocytosis that are all rescued by transfection of *ABP-120* (Cox et al., 1996).

CNS Roles of FLN1

While the critical role of FLN1 in neuronal migration is unexpected, FLN1's roles in nonneuronal cells form an obvious precedent for its neuronal role. Controlling the cross-linking of actin filaments, and repetitively forming and breaking focal adhesive contacts, are critical to the neuronal migration that characterizes the cerebral cortex. In response to deforming stress applied through $\beta 2$ integrin, cultured cells form extensive actin filaments via recruitment of actin by FLN1 (Glogauer et al., 1998), suggesting that FLN1 provides the direct link between membrane receptors and the actin cytoskeleton. Given that FLN1 is expressed in migrating cortical neurons, it is likely that it acts cell-autonomously in migrating neurons, though a role in radial glial cells cannot be completely ruled out.

FLN1's central role in binding both receptor and actin make it a prime candidate for being at the center of the signal transduction pathway that guides neuronal migration, with other signaling proteins implicated in neuronal migration, such as Dab1 and Cdk5/P35, likely to play regulatory roles. For example, Dab1 is an adapter protein with some homology to Shc and Numb, which both bind directly to membrane receptors (Howell et al., 1997). Since Dab1 appears to transduce a "stop" signal from the secreted ligand, Reelin (Rice et al., 1998), a simple model would have Dab1 blocking radial migration by disrupting FLN1 binding to a membrane receptor. The protein hypothetically bound by Dab1 and FLN1 would then be a candidate receptor for Reelin. Cdk5/P35 may also regulate the interaction of FLN1 with receptor via phosphorylation of the receptor-binding C terminus, since the CANSEARCH program (Songyang et al., 1995; Zhou and Cantley, 1995; Nishikawa et al., 1997) identifies many consensus phosphorylation sites for Cdk5/P35 (residues 2640, 2414, 1630, 2599, and 1148, all >97% probability) at the C terminus of FLN1. Hence, loss of Cdk5/P35 (Ohshima et al., 1996; Chae et al., 1997) function would resemble loss of Dab1 function.

FLN1's role in the CNS also likely involves migration of other neuronal types and perhaps axon outgrowth. The cerebellum is often subtly abnormal in PH, and additional CNS regions may be abnormal in hemizygous males. Moreover, neuronal migration and axon outgrowth bear considerable morphological similarities, and many of the genes involved in one are also involved in the other. Therefore, FLN1 would be an excellent candidate to control actin gelation and filopodia formation in growth cone extension. For example, cAMP regulates axon turning (Ming et al., 1997) and has long been known to control chemotaxis in *Dictylostelium discoideum* via regulation of the FLN1 homolog ABP-120 through a cAMP-dependent kinase (Cox et al., 1996). Chemotactic-like cAMP effects on axons could logically

be mediated by the known regulation of FLN1-dependent actin cross-linking via cAMP-dependent kinases. Abnormalities of the corpus callosum are common in PH (Table 1) and are likely to reflect defects in axonal connections, though an animal model will be needed to assess this clearly.

Finally, we note that all of the five *FLN1* alleles we have identified are consistent with complete loss of FLN1 function, representing either mutations at the most highly conserved residues required for proper splicing, nonsense mutations, or frameshift mutations. The typical female PH syndrome appears to correspond to the complete loss-of-function state, but milder alleles such as amino acid substitutions may ultimately be found to have milder phenotypes. Perhaps, some milder alleles such as the Xq28 duplication described above will be nonlethal, albeit neurologically severe, in males. Other associated findings might include hyper- or hypocoagulable states, vascular malformation, or dysmorphic features. Thus, *FLN1* mutations may ultimately represent a broad phenotypic spectrum with neurological and non-neurological manifestations.

Experimental Procedures

SSCP Analysis
Exons were amplified by PCR directly from genomic DNA of patients and controls with Qiagen (Valencia, CA) Taq polymerase according to the manufacturer's recommendations. Products were diluted 50:50 in SSCP loading buffer (95% formamide, 20 mM NaOH, 20 mM EDTA, 0.05% bromophenol blue, 0.05% xylene cyanol), incubated at 95°C for 5 min, and flash cooled on ice. Products were loaded onto nondenaturing, 0.5× MDE acrylamide gels (FMC Bioproducts, Rockland, ME) in 0.6× TBE and run at a constant 8 W for 16 hr at room temperature. Gels were stained with the Promega (Madison, WI) Silver Staining Kit according to the manufacturer's instructions.

DNA Sequencing
Normal and aberrantly migrating bands from the stained SSCP gels were covered with 1 μl polyacrylamide gel elution buffer (0.5 M ammonium acetate, 10 mM magnesium acetate, 1 mM EDTA [pH 8.0], 0.1% SDS), excised with a clean razor blade, macerated in an additional 25 μl elution buffer, and incubated at 37°C for >3 hr. Supernatant (0.5 μl) was used as template for PCR reactions to reamplify products from excised bands. These products, along with the original heterozygous products run on the SSCP gels, were gel purified (Geneclean Kit, Bio 101, Vista, CA) and sequenced with the Big Dye Cycle Sequencing Kit (Applied Biosystems, Foster City, CA) according to the manufacturer's protocol using the same primers used for the initial PCR reactions. Sequencing products were run on an ABI 377 automated sequencer and analyzed using the Sequencher program (GeneCodes, Ann Arbor, MI). All mutations were verified by reamplifying products from genomic DNA and repeating the SSCP analysis and sequencing.

Northern Analysis
Whole brains were extracted from E14, E16, P0, and adult mice, and RNA was extracted in TriReagent (Sigma, St. Louis, MO) according to the manufacturer's instructions. RNA (10 μg) from each sample was run on a denaturing 1% agarose gel for 5 hr at 7.5 V/cm. The gel was stained with ethidium bromide and photographed on a UV transilluminator. No significant degradation was observed for any sample, and clear 18 and 28S ribosomal bands were visible in each lane at roughly equal intensities. The RNA was transferred overnight by capillary action in 20× SSC to a positively charged nylon membrane (Hybond N+, Amersham, Piscataway, NJ) and fixed by UV cross-linking (120,000 J/cm²) and baking at 70°C for 1 hr. The 3' *FLN1* probe was labeled with [³²P]dCTP by random priming

(Oligolabelling Kit, Amersham) and hybridized to membranes in ExpressHyb solution (Clontech, Palo Alto, CA) according to the manufacturer's instructions. After exposure, the total RNA Northern blot was stripped by boiling for 1 min in 1% SDS and 0.1× SSC and reprobed with the G3PD probe.

Western Analysis

Western analysis of 50 μg total protein from fresh frozen human brain homogenates was performed according to protocols described in detail elsewhere (Bagrodia et al., 1995). The antibody used was the mouse monoclonal PM6/317 (Serotec, Raleigh, NC), raised against human FLN1. It was used at 1:20 dilution and developed with a goat anti-mouse secondary antibody and the Amersham Enhanced Chemiluminescence detection kit.

Immunohistochemistry

Immunofluorescence was performed on primary rat hippocampus (E15) and primary mouse cortex (E17) cells cultured in DMEM with 10% fetal calf serum. Cells were grown for 2–3 days and then briefly fixed with 4% methanol-free formaldehyde in a staining buffer containing 25 mM HEPES (pH 7.4), 2.5 mM KCl, 2.5 mM MgAc₂, and 250 mM sucrose. The cells were then blocked with 5 mg/ml lysine and 1% BSA and incubated for 1 hr with a mouse anti-human filamin monoclonal antibody (Chemicon International, Temecula, CA) at 1:500 dilution in the staining buffer containing 1% BSA and 0.25% of saponin. After the cells were washed in staining buffer, they were incubated with an anti-mouse secondary antibody conjugated to fluorescein (Jackson ImmunoResearch Laboratories, West Grove, PA) and then washed, coverslipped in Aquamount, and viewed under an Olympus fluorescent microscope. Negative controls, lacking primary antibody, showed no staining at all and hence are not illustrated.

Immunohistochemistry was performed on a postmortem specimen of human embryo (21–22 weeks gestation), fixed in formaldehyde, embedded in paraffin, and sectioned at 14 μm. Sections were deparaffinized in xylenes, rehydrated through a graded series of alcohol (100% for 10 min twice and then 95% for 5 min, 70% for 5 min, and 50% for 5 min), and then washed in PBS. Sections were blocked with 5% serum and 0.1% Triton X-100 in PBS for 1 hr and then incubated in primary antibody diluted in blocking solution for 2 hr. Sections were then washed three times in PBS and developed with a biotinylated secondary antibody and the ABC kit (Vector Laboratories, Burlingame, CA) according to the manufacturer's instructions.

X Inactivation

X inactivation patterns were analyzed using the HUMARA marker on DNA prepared from peripheral blood lymphocytes using standard techniques described elsewhere (Kopp et al., 1997). In brief, DNA samples were amplified using the HUMARA primers either unmodified or following digestion by HpaII, which digests a methylation-sensitive restriction enzyme cleavage site within the segment of DNA flanked by the HUMARA primers. Thus, the allele present on the transcriptionally active X chromosome is digested and is not amplified, while the transcriptionally inactive allele is not digested and is amplified efficiently. Biased X inactivation is thus manifested by preferential disappearance of one allele.

References

Bagrodia, S., Taylor, S., Creasy, C., Chernoff, J., and Cerione, R. (1995). Identification of a mouse p21Cdc42/Rac activated kinase. J. Biol. Chem. *270*, 22731–22737.

Bellanger, J., Zugasti, O., Lazaro, J., Diriong, S., Lamb, N., Sardet, C., and Debant, A. (1998). C. R. Seances Soc. Biol. Fil. *192*, 367–372.

Bugge, T., Xiao, Q., Kombrinck, K., Flick, M., Holmback, K., Danton, M., Colbert, M., Witte, D., Fujikawa, K., Davie, E., and Degen, J. (1996). Fatal embryonic bleeding events in mice lacking tissue factor, the cell-associated initiator of blood coagulation. Proc. Natl. Sci. USA *93*, 6258–6263.

Caviness, V.S., Jr., and Sidman, R.L. (1973). Time of origin or corresponding cell classes in the cerebral cortex of normal and reeler mutant mice: an autoradiographic analysis. J. Comp. Neurol. *148*, 141–151.

Chae, T., Kwon, Y., Bronson, R., Dikkes, P., Li, E., and Tsai, L. (1997). Mice lacking p35, a neuronal specific activator of Cdk5, display cortical lamination defects, seizures, and adult lethality. Neuron *18*, 29–42.

Condeelis, J., Vahey, M., Carboni, J., DeMey, J., and Ogihara, S. (1984). Properties of the 120,000- and 95,000-dalton actin-binding proteins from Dictyostelium discoideum and their possible functions in assembling the cytoplasmic matrix. J. Cell Biol. *99*, 119S–126S.

Cox, D., Wessels, D., Soll, D., Hartwig, J., and Condeelis, J. (1996). Reexpression of ABP-120 rescues cytoskeletal, motility, and phagocytosis defects of ABP-120 Dictyostelium mutants. Mol. Biol. Cell *7*, 803–823.

Cunningham, C., Gorlin, J., Kwiatkowski, D., Hartwig, J., Janmey, P., Byers, H., and Stossel, T. (1992). Actin-binding protein requirement for cortical stability and efficient locomotion. Science *255*, 325–327.

D'Adamo, P., Menegon, A., Lo Nigro, C., Grasso, M., Gulisano, M., Tamanini, F., Bienvenu, T., Gedeon, A., Oostra, B., Wu, S., et al. (1998). Mutations in GDI1 are responsible for X-linked nonspecific mental retardation. Nat. Genet. *19*, 134–139.

des Portes, V., Pinard, J., Billuart, P., Vinet, M., Koulakoff, A., Carrie, A., Gelot, A., Dupuis, E., Motte, J., Berwald-Netter, Y., et al. (1998). A novel CNS gene required for neuronal migration and involved in X-linked subcortical laminar heterotopia and lissencephaly syndrome. Cell *92*, 51–61.

Edwards, D., Towb, P., and Wasserman, S. (1997). An activity-dependent network of interactions links the Rel protein Dorsal with its cytoplasmic regulators. Development *124*, 3855–3864.

Ekşioğlu, Y.Z., Scheffer, I.E., Cardenas, P., Knoll, J., DiMario, F., Ramsby, G., Berg, M., Kamuro, K., Berkovic, S.F., Duyk, G.M., et al. (1996). Periventricular heterotopia: an X-linked dominant epilepsy locus causing aberrant cerebral cortical development. Neuron *16*, 77–87.

Fink, J., Dobyns, W., Guerrini, R., and Hirsch, B. (1997). Identification of a duplication of Xq28 associated with bilateral periventricular nodular heterotopia. Am. J. Hum. Genet. *61*, 379–387.

Gleeson, J., Allen, K., Fox, J., Lamperti, E., Berkovic, S., Cooper, E., Scheffer, I., Dobyns, W., Minnerath, S., Ross, M., and Walsh, C. (1998). *doublecortin*, a brain-specific gene mutated in human X-linked lissencephaly and double cortex syndrome, encodes a putative signaling protein. Cell *92*, 63–72.

Glogauer, M., Arora, P., Chou, D., Janmey, P., Downey, G., and McCulloch, C. (1998). The role of actin-binding protein 280 in integrin-dependent mechanoprotection. J. Biol. Chem. *275*, 1689–1698.

Gonzalez, J., Russo, C., Goldowitz, D., Sweet, H., Davisson, M., and Walsh, C. (1997). Birthdate and cell marker analysis of scrambler: a novel mutation affecting cortical development with a reeler-like phenotype. J. Neurosci. *17*, 9204–9211.

Gorlin, J., Yamin, R., Egan, S., Stewart, M., Sossel, T., Kwiatkowski, D., and Hartwig, J. (1990). Human endothelial actin-binding protein (ABP-280, nonmuscle filamin): a molecular leaf spring. J. Cell Biol. *111*, 1089–1105.

Hartwig, J. (1992). Mechanisms of actin rearrangements mediating platelet activation. J. Cell Biol. *106*, 1525–1538.

Hartwig, J., and Shevlin, P. (1986). The architecture of actin filaments and the ultrastructural location of actin-binding protein in the periphery of lung macrophages. J. Cell Biol. *103*, 1007–1020.

Hartwig, J., and Stossel, T. (1975). Isolation and properties of actin, myosin, and a new actin-binding protein in rabbit alveolar macrophages. J. Biol. Chem. *250*, 5696–5705.

Hartwig, J., Tyler, J., and Stossel, T. (1980). Actin-binding protein promotes the bipolar and perpendicular branching of actin filaments. J. Cell Biol. *87*, 841–848.

Howell, B., Gertler, F., and Cooper, J. (1997). Mouse disabled (mDab1): a Src binding protein implicated in neuronal development. EMBO J. *16*, 121–132.

Huttenlocher, P., Taravath, S., and Mojtahedi, S. (1994). Periventricular heterotopia and epilepsy. Neurology *44*, 51–55.

Just, W., Rau, W., Muller, R., Geerkens, C., and Vogel, W. (1994). Dinucleotide repeat polymorphism at the human biglycan (BGN) locus. Hum. Mol. Genet. *3*, 2268.

Kopp, P., Jaggi, R., Tobler, A., Borisch, B., Oestreicher, M., Sabacan, L., Jameson, J., and Fey, M. (1997). Clonal X inactivation analysis of human tumours using the human androgen receptor gene (HUMARA) polymorphism: a nonradioactive and semiquantitative strategy applicable to fresh and archival tissue. Mol. Cell. Probes *11*, 217–228.

Letourneau, P., and Shattuck, T. (1989). Distribution and possible interactions of actin-associated proteins and cell adhesion molecules of nerve growth cones. Development *105*, 505–519.

Loo, D., Kanner, S., and Aruffo, A. (1998). Filamin binds to the cytoplasmic domain of the β1-integrin. Identification of amino acids responsible for this interaction. J. Biol. Chem. *273*, 23304–23312.

Maestrini, E., Patrosso, C., Mancini, M., Rivella, S., Rocchi, M., Repetto, M., Villa, A., Frattini, A., Zoppe, M., Vezzoni, P., and Toniolo, D. (1993). Mapping of two genes encoding isoforms of the actin binding protein ABP-280, a dystrophin like protein, to Xq28 and to chromosome 7. Hum. Mol. Genet. *2*, 761–766.

Maestrini, E., Tamagnone, L., Longati, P., Cremona, O., Gulisano, M., Bione, S., Tamanini, F., Neel, B.G., Toniolo, D., and Comoglio, P.M. (1996). A family of transmembrane proteins with homology to the MET-hepatocyte growth factor receptor. Proc. Natl. Acad. Sci. USA *93*, 674–678.

Marti, A., Luo, Z., Cunningham, C., Ohta, Y., Hartwig, J., Stossel, T., Kyriakis, J., and Avruch, J. (1997). Actin-binding protein-280 binds the stress-activated protein kinase (SAPK) activator SEK-1 and is required for tumor necrosis factor-α activation of SAPK in melanoma cells. J. Biol. Chem. *272*, 2620–2628.

Matsudaira, P. (1994). Actin crosslinking proteins at the leading edge. Semin. Cell Biol. *5*, 165–174.

Meyer, S., Zuerbig, S., Cunningham, C., Hartwig, J., Bissell, T., Gardner, K., and Fox, J. (1997). Identification of the region in actin-binding protein that binds to the cytoplasmic domain of glycoprotein Ibα. J. Biol. Chem. *272*, 2914–2919.

Ming, G., Song, H., Berninger, B., Holt, C., Tessier-Lavigne, M., and Poo, M.-M. (1997). cAMP-dependent growth cone guidance by netrin-1. Neuron *19*, 1225–1235.

Murray, J.G. (1997). Mayo Clinic Cardiology Review (Armonk, NY: Futura Publishing).

Nishikawa, K., Toker, A., Johannes, F.J., Songyang, Z., and Cantley, L.C. (1997). Determination of the specific substrate sequence motifs of protein kinase C isozymes. J. Biol. Chem. *272*, 952–960.

Ohshima, T., Ward, J., Huh, C., Longenecker, G., Veeranna, Pant, H., Brady, R., Martin, L., and Kulkarni, A. (1996). Targeted disruption of the cyclin-dependent kinase 5 gene results in abnormal corticogenesis, neuronal pathology and perinatal death. Proc. Natl. Acad. Sci. USA *93*, 11173–11178.

Ohta, Y., and Hartwig, J. (1995). Actin filament cross-linking by chicken gizzard filamin is regulated by phosphorylation in vitro. Biochemistry *34*, 6745–6754.

Okita, J., Pidard, D., Newman, P., Montgomery, R., and Kunicki, T. (1985). On the association of glycoprotein Ib and actin-binding protein in human platelets. J. Cell Biol. *100*, 317–321.

Ott, I., Fischer, E., Miyagi, Y., Mueller, B., and Ruf, W. (1998). A role for tissue factor in cell adhesion and migration mediated by interaction with actin-binding protein 280. J. Cell Biol. *140*, 1241–1253.

Patrosso, M., Repetto, M., Villa, A., Milanesi, L., Frattini, A., Faranda, S., Mancini, M., Maestrini, E., Toniolo, D., and Vezzoni, P. (1994). The exon-intron organization of the human X-linked gene (*FLN1*) encoding actin-binding protein 280. Genomics *21*, 71–76.

Pfaff, M., Liu, S., Erle, D., and Ginsberg, M. (1998). Integrin β cytoplasmic domains differentially bind to cytoskeletal proteins. J. Biol. Chem. *273*, 6104–6109.

Reiner, O., Carrozzo, R., Shen, Y., Wehnert, M., Faustinella, F., Dobyns, W., Caskey, C., and Ledbetter, D. (1993). Isolation of a Miller-Dieker lissencephaly gene containing G protein β-subunit-like repeats. Nature *364*, 717–721.

Rice, D., Sheldon, M., D'Arcangelo, G., Nakajima, K., Goldowitz, D., and Curran, T. (1998). Disabled-1 acts downstream of reelin in a signaling pathway that controls laminar organization in the mammalian brain. Development *125*, 3719–3729.

Rogner, U., Heiss, N., Kioschis, P., Wiemann, S., Korn, B., and Poustka, A. (1996). Transcriptional analysis of the candidate region for incontinentia pigmenti (IP2) in Xq28. Genome Res. *6*, 922–934.

Sedlacek, Z., Korn, B., Konecki, D., Siebenhaar, R., Coy, J., Kioschis, P., and Poustka, A. (1993). Construction of a transcription map of a 300 kbp region around the human G6PD locus by direct cDNA selection. Hum. Mol. Genet. *2*, 1865–1869.

Shapiro, M.B., and Senapathy, P. (1987). RNA splice junctions of different classes of eukaryotes: sequence statistics and functional implications in gene expression. Nucleic Acids Res. *15*, 7155–7173.

Sharma, C., Ezzell, R., and Arnaout, M. (1995). Direct interaction of filamin (ABP-280) with the β2-integrin subunit. J. Immunol. *154*, 3461–3470.

Small, K., and Warren, S. (1998). Emerin deletions occurring on both Xq28 inversion backgrounds. Hum. Mol. Genet. *7*, 135–139.

Small, K., Iber, J., and Warren, S. (1997). Emerin deletion reveals a common X chromosome inversion mediated by inverted repeats. Nat. Genet. *16*, 96–99.

Songyang, Z., Carraway III, K., Eck, M., Harrison, S., Feldman, R., Mohammadi, M., Schlessinger, J., Hubbard, S., Smith, D., Eng, C., et al. (1995). Catalytic specificity of protein-tyrosine kinases is critical for selective signaling. Nature *373*, 536–539.

Stendahl, O., Hartwig, J., Brotschi, E., and Stossel, T. (1980). Distribution of actin-binding protein and myosin in macrophages during spreading and phagocytosis. J. Cell Biol. *84*, 215–224.

Wang, K., Ash, J., and Singer, S. (1975). Filamin, a new high-molecular-weight protein found in smooth muscle and nonmuscle cells. Proc. Natl. Acad. Sci. USA *72*, 4483–4486.

Wang, Q., Patton, W., Chiang, E., Hechtman, H., and Shepro, D. (1996). Filamin translocation is an early endothelial cell inflammatory response to bradykinin: regulation by calcium, protein kinases, and protein phosphatases. J. Cell Biochem. *62*, 383–396.

Ware, J., Russell, S., Vicente, V., Scharf, R., Tomer, A., McMillan, R., and Ruggeri, Z. (1990). Nonsense mutation in the glycoprotein Ib α coding sequence associated with Bernard-Soulier syndrome. Proc. Natl. Acad. Sci. USA *87*, 2026–2030.

Zhang, W., Han, S., McKell, D., Goate, A., and Wu, J. (1998). Interaction of presenilins with the filamin family of actin-binding proteins. J. Neurosci. *18*, 914–922.

Zhou, S., and Cantley, L.C. (1995). Recognition and specificity in protein tyrosine kinase-mediated signaling. Trends Biochem. Sci. *20*, 470–475.